PREPARATION OF SUPERCONDUCTING WIRE BY DEPOSITION OF $YBa_2Cu_3O_x$ ONTO FIBERS

W.J. Lackey, J.A. Hanigofsky, M.J. Shapiro,
W.B.Carter, D.N. Hill, E.K. Barefield, E.A. Judson,
D.F. O'Brien, Y.S. Chung, and T.S. Moss
Georgia Institute of Technology
Atlanta, Georgia 30332

and

K.L. More
Oak Ridge National Laboratory
Oak Ridge, Tennessee 37830

A controllable process has been developed for chemical vapor deposition of superconducting $YBa_2Cu_3O_x$. The process relies on feeding and transport of a finely ground powder mixture of Y, Ba, and Cu tetramethylheptanedionates into a CVD furnace. X-ray diffraction, scanning electron microscopy, analytical electron microscopy, resistance versus temperature, and critical current measurements have been used to characterize the films. The optimum processing parameters were determined using parametric studies involving temperature, pressure, reagent feed rate and composition, and coating time. Extensive c-axis orientation was observed using x-ray diffraction and transmission electron microscopy. The presence of impurity phases and substrate/coating interaction layers were observed. $YBa_2Cu_3O_x$ coatings on MgO (100) single crystal substrates exhibited critical currents of 2×10^4 A/cm^2 at 77 K, 0 Tesla, with critical temperatures (Resistance=0) of 86 K. Deposition of the $YBa_2Cu_3O_x$ material onto several fibrous substrates has been achieved, and a continuous fiber coating furnace is in operation.

INTRODUCTION

Chemical vapor deposition (CVD) of ceramic superconductors has recently received attention by several researchers. CVD offers unique advantages over other processing methods, including higher quality, more adherent films, with the specific advantage of coating irregularly shaped objects, including infiltration and coating of multifilament fiber tows. Over a dozen investigators have reported on the CVD of superconducting $YBa_2Cu_3O_x$ (1-23); a summary of these results is presented in Table I. Some of these films have very high critical current densities (10^5 A/cm^2 at 0 Tesla, 77 K) even in strong magnetic fields (10^4 A/cm^2 at 27 Tesla, 77 K) (17,19).

Most of the studies summarized in Table 1 used metal complexes of various β-diketonate ligands. These solids slowly sublime when heated to 100-300°C, and are carried into the furnace using an optimal flow rate of a carrier gas (usually argon). This is the conventional vaporizer approach used in CVD. To obtain the desired $YBa_2Cu_3O_x$ molar ratio, precise control of vaporizer temperature, pressure, and carrier gas flow rate for each reagent solid is required. The deposition is further complicated by the very low vapor pressures of the Y, Ba, and Cu precursor reagents and their strong temperature dependence. Thermally induced decomposition of the barium reagents has been reported as a specific processing problem with this approach (6,16).

In the powder feeding process described here (24), a mixture of the three solid reagents is fed directly into the coating furnace where the reagents vaporize and subsequently undergo the deposition reaction(s). This method reduces the process control variables and results in a faster, potentially more economical CVD process. Process repeatability is enhanced, and the growth rates have been increased nearly two orders of magnitude over conventional vaporizer processing (200 μm h vs 1-10 μm/h). The extension of this deposition technology to continuous lengths of flexible ceramic fibers is being studied in order to fabricate a prototype high temperature superconducting magnet.

EXPERIMENTAL PROCEDURE

The deposition of $YBa_2Cu_3O_x$ thin films was accomplished in a low pressure, hot walled CVD reactor as shown in Figure 1. The precursors were the β-diketonate complexes $Y(tmhd)_3$, $Ba(tmhd)_2$, and $Cu(tmhd)_2$. The yttrium and copper complexes were prepared by minor modifications of literature procedures (25,26) and were recrystallized from hexane before use. The barium complex was prepared by reaction of 2,2,6,6-tetramethyl-3,5-heptanedione with barium metal at 100°C, followed by dissolution in toluene and precipitation with acetonitrile at room temperature. The solid reagents were premixed and ground in air using a Spex model 8000 Mixer/Mill; the particles were subsequently screened below 44 μm.

A powder feeder was used to slowly introduce the powder reagent mixture into the CVD furnace. Ultra High Purity argon was used to pneumatically transport the mixture to the furnace where it vaporized and then reacted to deposit on the hot substrate. Ultra High Purity oxygen, which was pretreated with CuO at 500°C, Ascarite, and Drierite to reduce the CO_2 and H_2O impurities, was added to the inlet gas stream near the furnace. Gas flow rates were controlled using MKS mass flow controllers; the temperature was monitored using an Inconel sheathed Type K thermocouple. Immediately following deposition, the samples were furnace cooled to 300°C in 1 atm O_2 flowing at 1 ℓ/min. Coatings were deposited on several flat substrates including single crystals of MgO, $SrTiO_3$, and stabilized ZrO_2 and polycrystals of Al_2O_3, Ag, and stabilized ZrO_2. Fibrous substrates evaluated were Sumitomo, Nicalon, Nextel, Ag, Saphikon (single crystal Al_2O_3) and FP Alumina.

CHARACTERIZATION

X-ray diffraction (XRD) of the films was performed using a Philips PW-1800 Automated Powder Diffractometer equipped with a rotating sample stage. The samples were analyzed using monochromatic copper K_α radiation, at tube voltage/current settings of 40 kV/30 mA. The samples were scanned from 10 to 70° 2θ, which encompassed most of the major peaks of interest. Lattice parameter estimations of the $YBa_2Cu_3O_x$ unit cell were determined by using an interactive computer program which calculates precise lattice parameters of a known phase using a set of reflections and a good initial estimate of the lattice parameters.

Chemical and microstructural analyses of the coatings were performed using a CWIKSCAN Model 104 scanning electron microscope equipped with a KEVEX Model 7500 energy-dispersive x-ray (EDS) analyzer. All quantitative chemical analyses were accomplished on flat substrates in the as-annealed condition and were compared to a bulk $YBa_2Cu_3O_x$ standard.

Cross-sections of the films were prepared for transmission electron microscopy (TEM) by gluing two coatings face-to-face and subsequently cutting slices from this

"sandwich." Each specimen was then subjected to mechanical thinning to 75 μm, dimpling, and ion milling using 6 kV argon ions. Ion milling was performed using a liquid nitrogen cooled stage to minimize damage to the superconducting film. Samples were examined in a JEOL 2000FX operated at 200 kV. High resolution images were recorded in a JEOL 4000X operated at 400 kV. All photographs were taken near Scherzer defocus (-50 nm) and a convergence of 1 mr.

Resistance versus temperature measurements were made utilizing the four point probe method. Silver contacts were evaporated onto the specimens which were subsequently annealed in one atmosphere of oxygen for one hour at 500°C. Thin copper wires were attached with conductive epoxy. Specimens were mounted on a cold finger capable of temperatures as low as 10 K. Specimen temperatures were monitored with a silicon diode. Both AC and DC techniques were used with currents as low as 10 μA. Critical current densities were measured on flat substrates by physically "etching" the coating to form a current constricting path between the inner pair of silver contacts. The constrictions were about 0.5 mm wide by about 5 mm long. The samples were immersed in liquid nitrogen (77 K) at 0 Tesla. The critical current density was defined by that current density required to produce an electric field of 1.0 μV/cm.

RESULTS

Optimization studies included over 200 coating runs where the major processing variables were adjusted over the ranges given in Table II. The preferred conditions selected were the result of statistically designed experiments which studied the effects of temperature, pressure, reagent concentration and feed rate, and oxygen and argon flow rates on the film structure, composition, and electrical properties. The unique reagent introduction system resulted in deposition rates approaching two orders of magnitude greater than those achieved using the conventional CVD technique (eg., 200 μm/h vs 1-10 μm/h). A maximum deposition rate of 240 μm/h was achieved.

The coatings were smooth, black, uniform, and adherent to the substrate. Most coatings on planar substrates showed extensive preferred orientation, with the c-axis of the $YBa_2Cu_3O_x$ coating perpendicular to the substrate surface. A typical x-ray diffraction pattern and SEM micrograph of the surface morphology of an $YBa_2Cu_3O_x$ film deposited on MgO are shown in Figures 2 and 3, respectively. The surface of the samples appeared flat, with some indication of plate-like c-axis oriented grains. The x-ray patterns were typically strongly (00ℓ) oriented, however, impurity phases including CuO, $BaCuO_2$, and the 211 phase (Y_2BaCuO_x) were present at lower intensities. The EDS analysis of the films consistently agreed with the XRD patterns; samples with low Y contained some CuO and $BaCuO_2$. Lattice parameter calculations indicated that a highly oxygenated orthorhombic structure was achieved. Typical lattice parameter values were a = 3.823 Å, b = 3.887 Å, and c = 11.683 Å.

Transmission electron microscopy also showed the strong c-axis orientation with respect to the substrate, as shown in Figure 4. Inset on Figure 4 is an electron diffraction pattern which indicates the c-axis direction. A high magnification TEM micrograph showing the c-axis orientation of the films is presented in Figure 5. Transmission electron microscopy and EDS were both used to identify impurity phases in the films, as shown in Figure 6. Both CuO and 211 grains, surrounded by the $YBa_2Cu_3O_x$ compound, were present in the films; Figure 6 shows several 211 grains surrounded by $YBa_2Cu_3O_x$. Interaction layers were also observed at the film/substrate interface for samples prepared on Al_2O_3 and stabilized ZrO_2 substrates. A barium aluminate phase and a barium zirconate phase were present at each

respective interface in Figures 7 and 8. No substrate coating interaction was observed by TEM for samples grown on MgO substrates.

Figure 9 shows six resistance versus temperature curves (solid lines) for early trials using the powder feeding method, and four curves (dashed lines) for runs conducted with optimized parameters. Critical temperatures of 80 K or above were achieved at the optimum conditions. The highest critical temperature and critical current density (zero field at 77 K) found on MgO have been 86 K and 2 x 10^4 A/cm^2, respectively. Figure 10 presents the critical current measurement for a $YBa_2Cu_3O_x$ film on single crystal yttria stabilized ZrO_2. At 1 $\mu V/cm$, the film had a current density of 3.6 x 10^4 A/cm^2. The critical temperature was 87 K.

Fibers were also coated in the horizontal furnace along with flat substrates. Both tows and monofilaments were found to contain $YBa_2Cu_3O_x$ by XRD. A coated Saphikon (single crystal alumina) fiber had a critical temperature of 82 K as shown in Figure 11.

The coating of continuous flexible ceramic fibers has been initiated. The coating furnace is shown in Figure 12. Fibrous tows are introduced at the bottom of the furnace from a supply spool, and are slowly pulled through the furnace and are wound on a takeup spool at the top. Figure 13 shows three fibers from a FP Alumina fiber tow (200 individual filaments) which were coated in the continuous fiber coating furnace. The coating appears uniform and adherent to the fiber; EDS analysis indicated the presence of Y, Ba, and Cu in the coating. Further work on optimization of the powder feed rate, fiber pull rate, and coating composition is underway.

DISCUSSION

The powder feeding of a mixture of Y, Ba, and Cu organometallic reagents has resulted in a CVD process which allows rapid deposition of superconducting $YBa_2Cu_3O_x$. Our experience was that it was much easier to repeatedly achieve superconducting $YBa_2Cu_3O_x$ with this technique than with the conventional vaporizer method as a result of a reduction in the processing variables and the elimination of thermal degradation of the precursors previously reported (6,16).

Several factors indicate the films were deposited by a vapor deposition mechanism, as opposed to powder spraying. First, we were able to infiltrate and uniformly coat individual fibers in a multifilament tow. Second, the films are very dense and smooth; imperfections such as film roughness and uneven coatings occurred only when the sample was placed too close to the inlet of the furnace. Finally, when coating multiple substrates placed behind one another, there were no appreciable differences in the coating, i.e., there was no shadowing effect.

Characterization of the films has shown the high c-axis orientation with respect to the substrate which is typical of other CVD efforts. Films deposited on both single crystal and polycrystalline materials have been shown to be superconducting. Transmission electron microscopy analysis has been useful in analyzing interfacial layers and showing the presence of impurity phases in the films. Of the two interaction layers observed, only the barium aluminate interface detrimentally affected the properties of the superconductor. This problem was overcome by depositing thicker coatings which the powder feeding process allows. The values of critical temperatures and critical current densities are acceptable; however, these properties must be increased through further process development.

CONCLUSIONS

A rapid, controllable CVD process has been developed which has been used to deposit superconducting $YBa_2Cu_3O_x$ on several single crystal, polycrystal, and fiber substrates. Process development has led to improvements in the electrical properties of the films, with critical temperatures as high as 87 K and critical currents of 3.6 x 10^4 A/cm^2 at 77 K, 0 Tesla. Microstructural characterization has shown a smooth surface morphology, with a highly c-axis oriented structure. TEM analysis has shown impurity phases including 211 and CuO grains, and interfacial layers between the substrate and coating. The process is currently being developed in conjunction with a continuous fiber coating furnace, in order to deposit the superconducting $YBa_2Cu_3O_x$ material onto long lengths of fiber tows for potential magnet, motor, antennae, and other applications.

ACKNOWLEDGMENTS

Funded by Dr. Frank Patten of the Defense Advanced Research Projects Agency and Dr. Wallace Smith of the Office of Naval Research. We acknowledge Dr. Garth Freeman for performing some of the scanning electron microscopy. The transmission electron microscopy was funded by the High Temperature Superconductivity Pilot Center Program, Office of Utility Technologies, Conservation and Renewable Energy, U.S. Department of Energy, under contract DE-AC05-84OR21400 with Martin Marietta Energy Systems, Inc., and was carried out at the Material Analysis Users Center, High Temperature Materials Laboratory, Oak Ridge National Laboratory.

REFERENCES

1. A. Berry, D. Gaskill, R. Holm, E. Cukauskas, R. Kaplan, and R. Henry, Appl. Phys. Lett., 52, 1743-1745 (1988)
2. H. Yamane, H. Kurosawa, and T. Hirai, Chemistry Lett., Issue No. 6, 939-940 (1988)
3. C. Gonzalez, O. Schachner, H. Tippmann, and F. Trojer, Physica C, 153-155, 1042-1043 (1988)
4. T. Nakamori, H. Abe, T. Kanamori, and S. Shibata, Jap. J. of Appl. Phys., 27, L1265-1267 (1988)
5. A. Panson, R. Charles, D. Schmidt, J. Szedon, G. Machiko, and A. Braginski, Appl. Phys. Lett., 53, 1756-1758 (1988)
6. K. Shinohara, F. Munakata, and M. Yamanaka, Jap. J. Appl. Phys., 27, L1683-1685 (1988)
7. J. Zhao, K. Dahmen, H. Marcy, L. Tonge, T. Marks, B. Wessels, and C. Kannewurf, Appl. Phys. Lett., 53, 1750-1752 (1988)
8. H. Yamane, H. Masumoto, T. Hirai, H. Iwasaki, K. Watanabe, N. Kobayashi, and Y. Muto, Appl. Phys. Lett., 53, 1548-1550 (1988)
9. K. Zhang, B. Kwak, E. Boyd, A. Wright, and A. Erbil, Appl. Phys. Lett., 54, 380-382 (1989)
10. K. Watanabe, H. Yamane, H. Kurosawa, T. Hirai, N. Kobayashi, H. Iwasaki, K. Noto, and Y. Muto, Appl. Phys. Lett., 54, 575-577 (1989)
11. S. Oda, H. Zama, T. Ohtsuka, K. Sugiyama, and T. Hattori, Jap. J. of Appl. Phys., 28, L427-429 (1989)
12. T. Tsuruoka, H. Takahashi, R. Kawasaki, and T. Kanamori, Appl. Phys. Lett., 54, 1808-1809 (1989)
13. M. Ottosson, T. Andersson, J. Carlsson, A. Harsta, U. Jansson, P. Norling, K. Niskanen, and P. Nordblad, Appl. Phys. Lett., 54, 2476-2478 (1989)
14. H. Yamane, H. Kurosawa, and T. Hirai, Proc. 7th European Conf. on CVD, Colloque De Physique, C-5, 131-140 (1989)

15. F. Schmaderer and G. Wahl, Proc. 7th European Conf. on CVD, Colloque De Physique, C-5, 119-129 (1989)
16. P. Dickenson, T. Geballe, A. Sanjurjo, D. Hildenbrand, G. Craig, M. Zisk, J. Collman, S. Banning, and R. Sievers, J. Appl. Phys., 66, 444-447 (1989)
17. H. Yamane, H. Kurosawa, T. Hirai, K. Wanatabe, H. Iwasaki, N. Kobayashi, and Y. Muto, Supercond. Sci. Technol., 2(2), 115-117 (1989)
18. F. Radpour, R. Singh, S. Sinha, A. Tulpule, P. Chou, R. Thakur, M. Rahmati, N. Hsu, and A. Kumar, Appl. Phys. Lett., 54(24), 2479-2480 (1989)
19. T. Hirai, H. Yamane, H. Kurosawa, K. Watanabe, N. Kobayashi, H. Iwasaki, and Y. Muto, 1989 International Superconductivity Electronics Conference (ISEC '89), June 12-13, 1989, Tokyo, Japan
20. K. Kanehori, N. Sugii, and K. Miyauchi, Journal of Solid State Chemistry, 82, 103-108 (1989)
21. Y. K. Rao and S. S. Kim, Journal of Superconductivity, 2(3), 395-407 (1989)
22. M. Inove, E. Takase, Y. Takai, and H. Hayakawa, Japanese Journal of Applied Physics, 28(9), L1575-1577 (1989)
23. T. Yamaguchi, S. Aoki, N. Sadakata, O. Kohno, and H. Osanai, Applied Physics Letters, 55(15), 1581-1582 (1989)
24. Patent pending.
25. K. J. Eisentraut and R. E. Sievers, J. Am. Chem. Soc., 87, 5254 (1965)
26. G. S. Hammond, D. Nonhebel, and C. Wu, Inorg. Chem., 2, 73 (1963)

Table I. Summary of prior CVD of $YBa_2Cu_3O_x$.

REFERENCE	GROUP	REAGENTS*	SUBSTRATE	TEMP(°C)	RATE(μm/h)	T_c(ONSET)(K)	T_c(R=0)(K)	ANNEAL CONDITIONS
1.	NRL	Y,Ba-tmhd Cu-acac	MgO	400	0.48	80	20	890-920°C 20 min, 920°C-10 min, 0.83°C/min in O_2
2.	TOHOKU	tmhd	YSZ	900	0.8	43	--	10 torr O_2
						83	33	400°C, O_2, 8 h
						90	62	30°C/min, 1 atm O_2
						89	80	3°C/min, 1 atm O_2
3.	BATTELLE	Cu-acac Y-tmhd Ba-hfa	YSZ	900				--
4.	OKI	tmhd	MgO	600	2.4 - 6	76	60	950°C 30 min, 2°C/min in O_2
5.	WESTING-HOUSE	Y,Ba-hfa Cu-acac	Sapphire $SrTiO_3$ Al_2O_3		5	90 90	65 70 65	H_2O/Ar 835°C 30 min, 900°C-10 min Ar, 8.3°C/min to-400°C, 400°C 30 min,-8.3°C/min to 200°C
6.	NISSAN	Y-tmhd Ba,Cu-hfa	$SrTiO_3$	600	0.33	83	65	850°C 2 h, 2°C/min to-500°C, 500°C 2 h,-2°C/min to RT (all in air)
7.	NORTH-WESTERN	Y-tmhd Cu-acac Ba-fod	MgO	700	0.6 - 1.8	90	66.2	600°C 10 h, 900°C 1.5 h-960°C 10 min in O_2
8.	TOHOKU	tmhd	$SrTiO_3$	900	2	88	84	15°C/min, 1 atm O_2
9.	GEORGIA TECH	tmhd	YSZ Sapphire	650	10	93 --	84 10	950°C 30 min, 4°C/min 895°C 15 min, 4°C/min in O_2
10.	TOHOKU	tmhd	$SrTiO_3$	850	1	-- 89	91.5	90°C/min, 1 atm O_2
11.	TOKYO IT/ MUSASHI	Cu-acac Y,Ba-hfa	Sapphire Si	500 700 500	0.3 - 0.9			
12.	OKI	tmhd	$SrTiO_3$	800	0.9	88 75 92	83 60	100°C/min in atm O_2 quenched to RT in 5s
13.	UPPSALA	YCl_3 BaI_2 CuCl	CSZ CSZ	870-910	3	80 80	40 70	-- 475°C 48 h in O_2

Table I. Summary of prior CVD of $YBa_2Cu_3O_x$ (continued).

REFERENCE	GROUP	REAGENTS*	SUBSTRATE	TEMP(°C)	RATE(μm/h)	T_c(ONSET)(K)	T_c(R=0)(K)	ANNEAL CONDITIONS
14.	TOHOKU	tmhd	YSZ	800	0.8 - 1	60	10	10 torr O_2
						80	30	450°C, 1 atm O_2, 1 h
						83	43	1 atm O_2
15.	ASEA	Cu-acac	$SrTiO_3$	900	0.6	94	88	20 min cool 1 atm O_2
	BROWN BAVERIA	Y,Ba-tmhd	YSZ	950		94	86	
16.	STANFORD/ SRI/COLO	tmhd	$SrTiO_3$	800	0.1 - 1	90	70	550°C 2 h
				900		87	77	
						70	64	
17.	TOHOKU	tmhd	YSZ	900	1 - 4	40	--	15°C/min, 10 torr O_2
						90	87	15°C/min, 1 atm O_2
			$SrTiO_3$				84	
				850			93	
				800			91	
18.	OKLAHOMA	tmhd	YSZ(BaF_2)	780	--	90	80	3.3°C/min Ar/O_2 to 400°C,-
			YSZ			90	50	2.5°C/min to 100°C
19.	TOHOKU	tmhd	YSZ	900	1 - 2			20°C/min, 1 atm O_2-
			Al_2O_3 Sapphire					to 300°C, quench
20.	HITACHI	$Y(tmhd)_3$	$MgO/SrTiO_3$	800	1.3	84	82	in situ cooling
		$Ba(tmhd)_2$	$MgO/SrTiO_3$	750	0.92	85	78	1 atm O_2, 20°C/min
		$Cu(tmhd)_2$	$SrTiO_3$	700	0.83	84	60	
			MgO	700	0.83	84	66	
			$MgO/SrTiO_3$	650	0.55			
21.	UNIV WASH (theoret- ical)	YCl_3	MgO	827	4.8			
		$BaCl_2$			39			
		CuCl						
22.	NAGOYA	$Y(dpm)_3$	MgO	663	1	<60K		in situ cooling, 5°C/min
		$Ba(dpm)_2$		715		89	<60K	to 400°C, 0.2 torr O_2, to
		$Cu(dpm)_2$		740		89	57	RT, 2 torr O_2
23.	FUJIKARA	$Y(tmhd)_3$	$SrTiO_3$	750	15-30	92	89	cooled to 500°C, 10 torr
		$Ba(tmhd)_2$	Hastelloy C-276			92	81	O_2, 500°C 3 h, 1 atm O_2
		$Cu(tmhd)_2$	Hastelloy C-276-$SrTiO_3$			92	84	

* tmhd= tetramethylheptanedionate
acac= acetylacetonate
dpm= dipiraloylmethanate
hfa= hexafluoroacetylacetonate
fod= heptafluorodimethyloctanedionate

Table II. Range of processing parameters investigated and preferred deposition conditions.

	RANGE INVESTIGATED	PREFERRED CONDITIONS
TOTAL PRESSURE (torr)	10-760	20
DEPOSITION TEMPERATURE (°C)	500-970	900
ARGON FLOW RATE (ℓ/min)	0-5	5
OXYGEN FLOW RATE (ℓ/min)	1-5	1
DEPOSITION TIME (min)	5-55	30
INPUT REAGENT MOLE RATIO $Y(tmhd)_3$:$Ba(tmhd)_2$:$Cu(tmhd)_2$	1:(1.58-2.55):(2.24-3.80)	1:1.75:2.25
TOTAL REAGENT MASS (g)	1-10	1.75

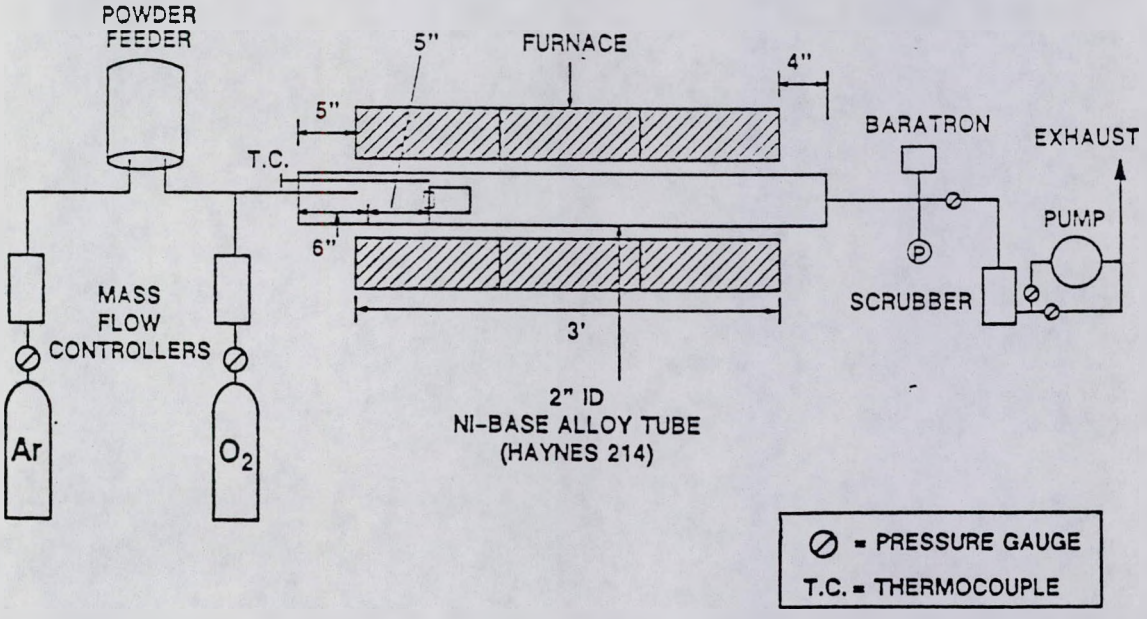

Figure 1. Schematic diagram of the CVD system.

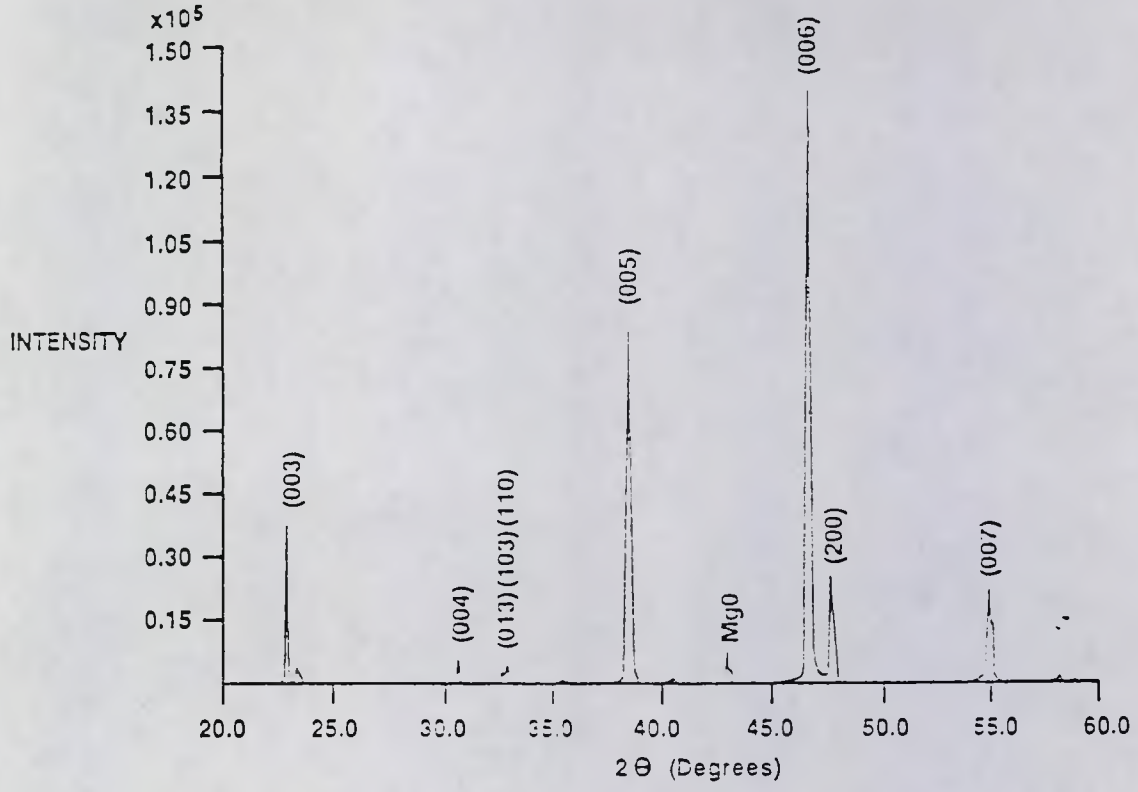

Figure 2. X-ray diffraction pattern for a $YBa_2Cu_3O_x$ film on MgO deposited at the preferred conditions.

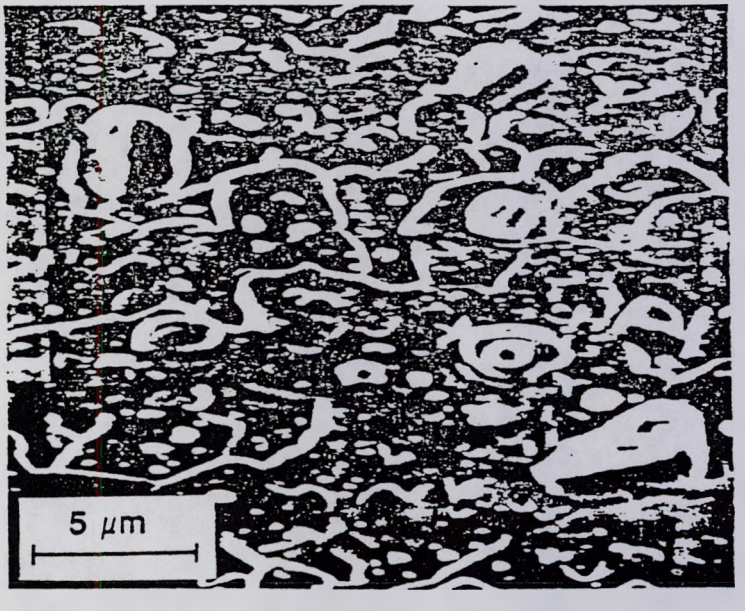

Figure 3. Typical $YBa_2Cu_3O_x$ film morphology on MgO shows a flat surface with some plate-like features.

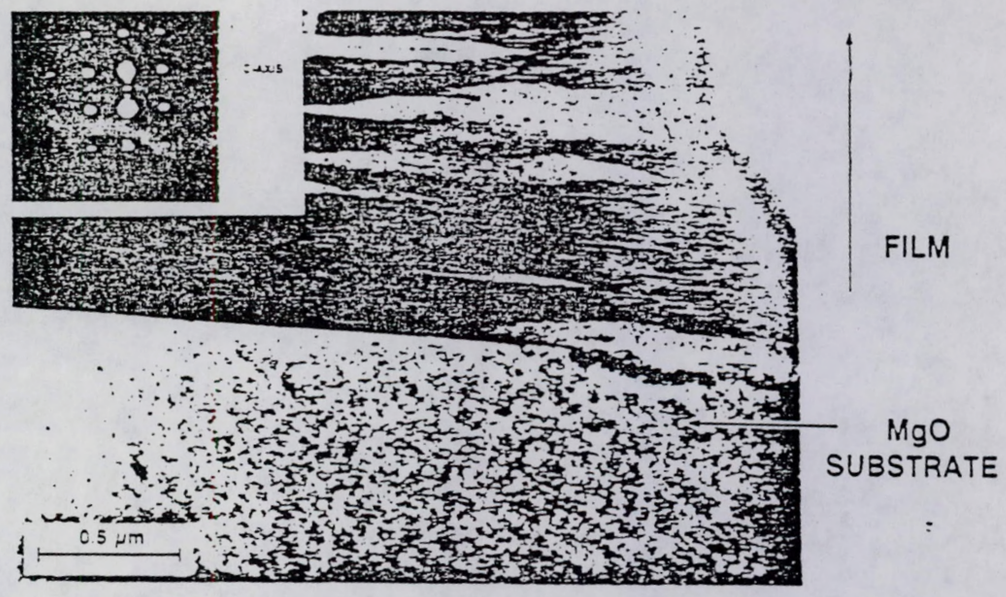

Figure 4. High resolution TEM shows c-axis orientation parallel to the MgO substrate. The electron diffraction pattern (inset) indicates the c-axis orientation.

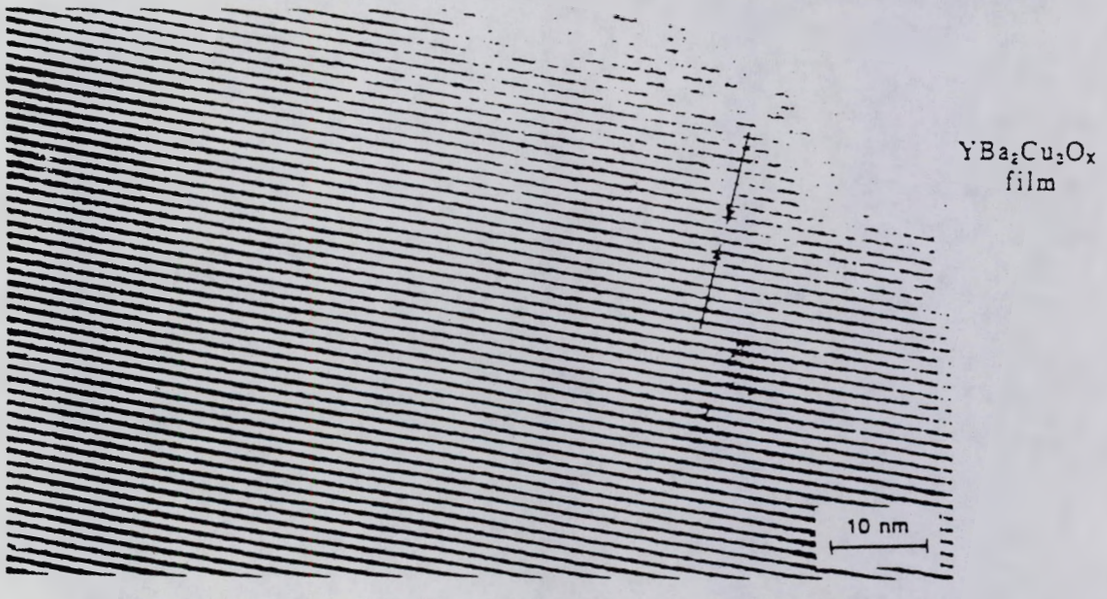

Figure 5. High magnification TEM shows the lattice spacing of the $YBa_2Cu_3O_x$ thin film.

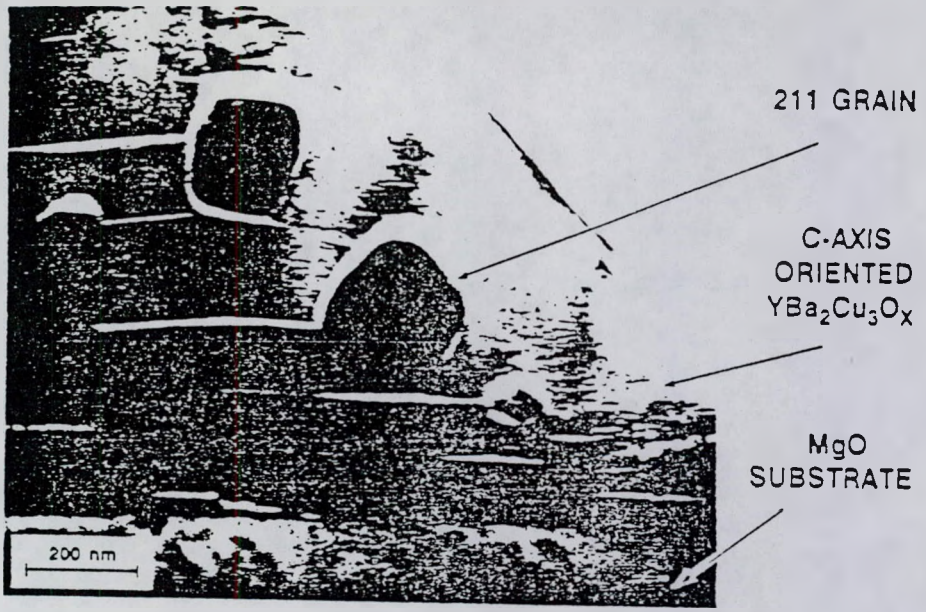

Figure 6. Impurity 211 grains were present in the films as shown by TEM and verified by EDS. CuO grains were seen in other films.

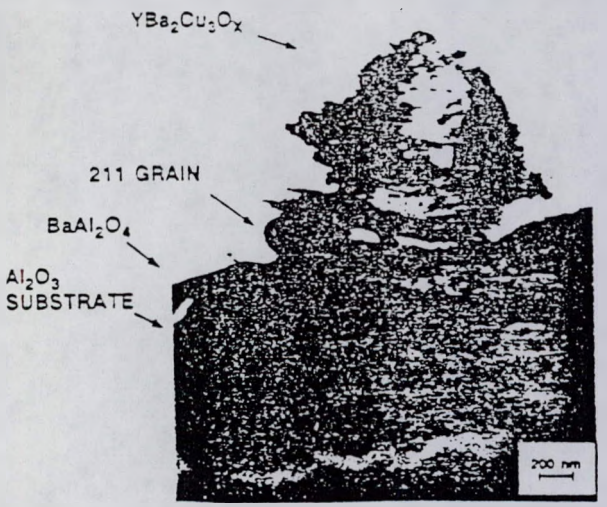

Figure 7. A barium aluminate interfacial layer was present in films deposited on Al_2O_3.

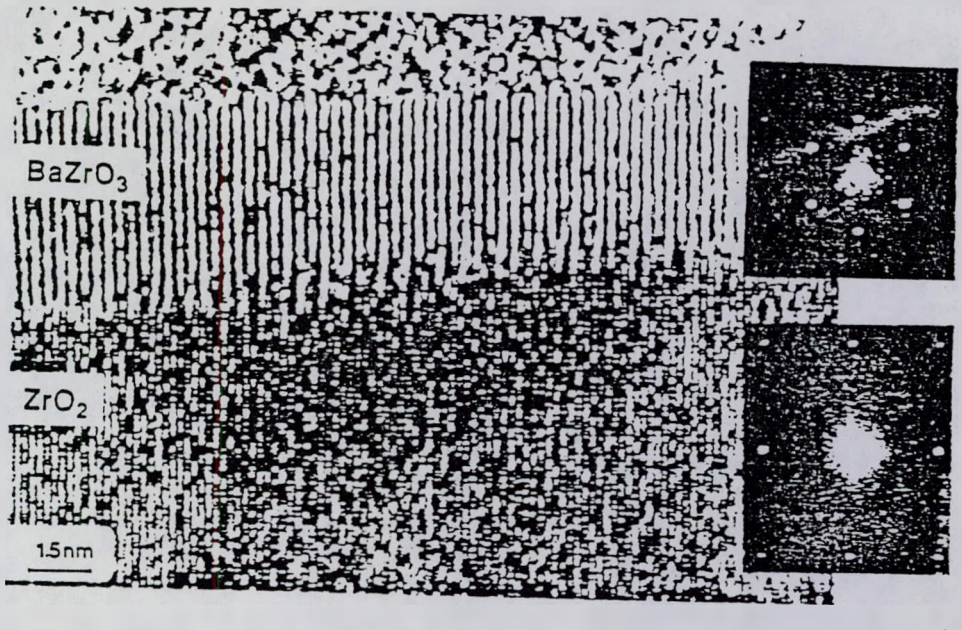

Figure 8. High resolution TEM was used to identify a barium zirconate interlayer between the $YBa_2Cu_3O_x$ film and single crystal partially stabilized ZrO_2. Electron diffractograms (inset) were used to verify each phase.

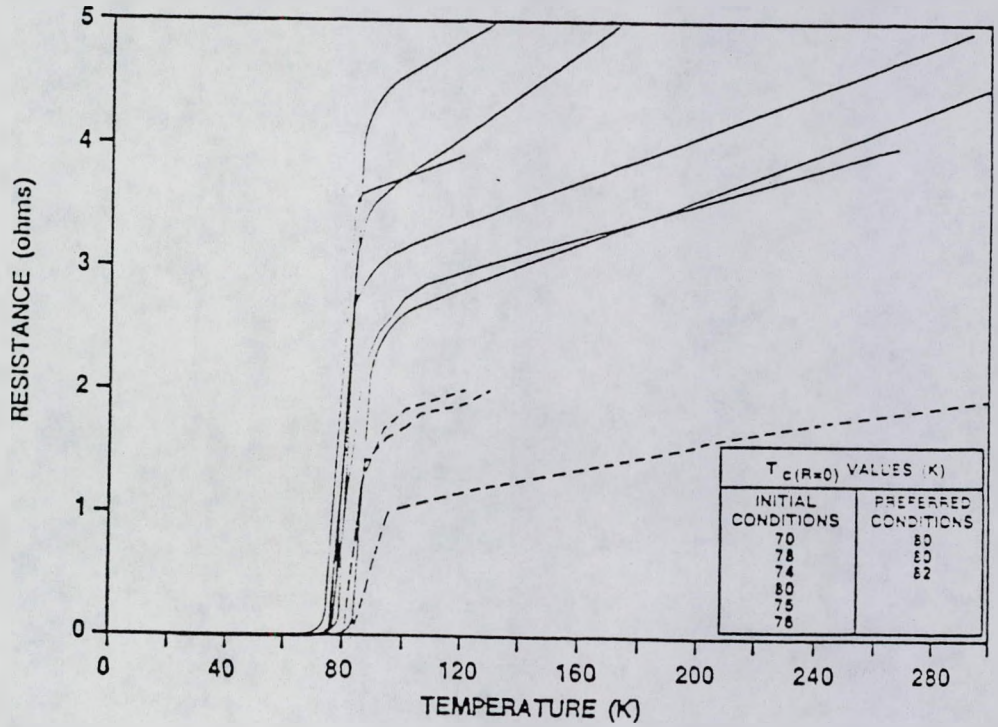

Figure 9. Resistance versus temperature curves for $YBa_2Cu_3O_x$ coatings on MgO substrates. The solid lines represent films deposited prior to the parametric studies, the dashed lines represent films deposited at the preferred conditions.

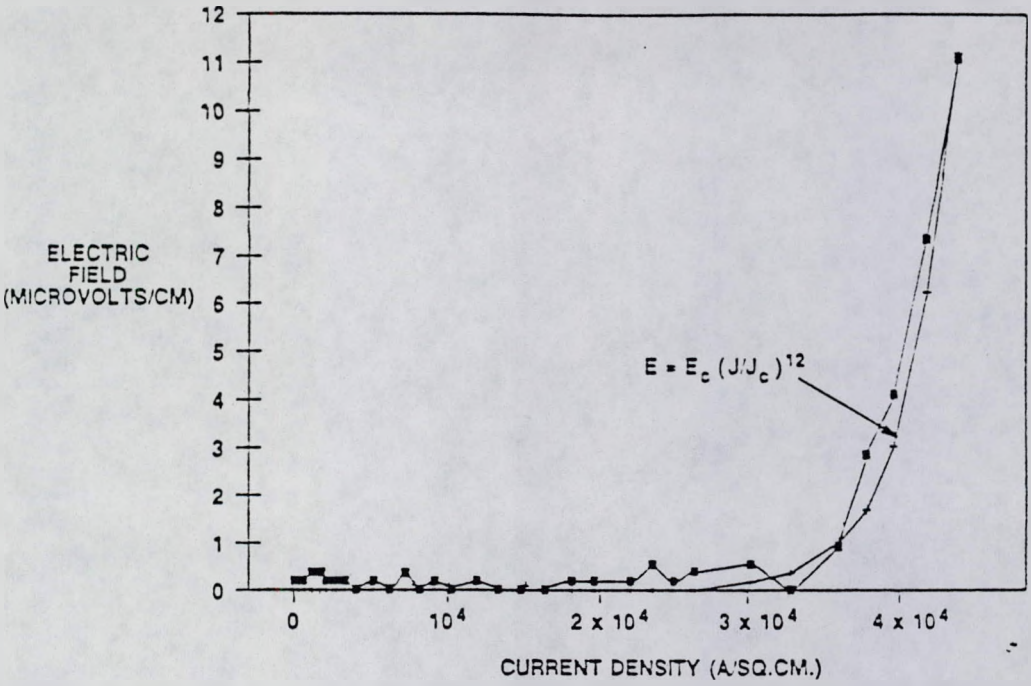

Figure 10. Electric field (E) versus current density (J) data of a film on single crystal stabilized ZrO_2. The crosses indicate a curve fit to the data where $E_C = 1\ \mu V/cm$ and $J_C = 3.6 \times 10^4\ A/cm^2$. The squares represent the actual data.

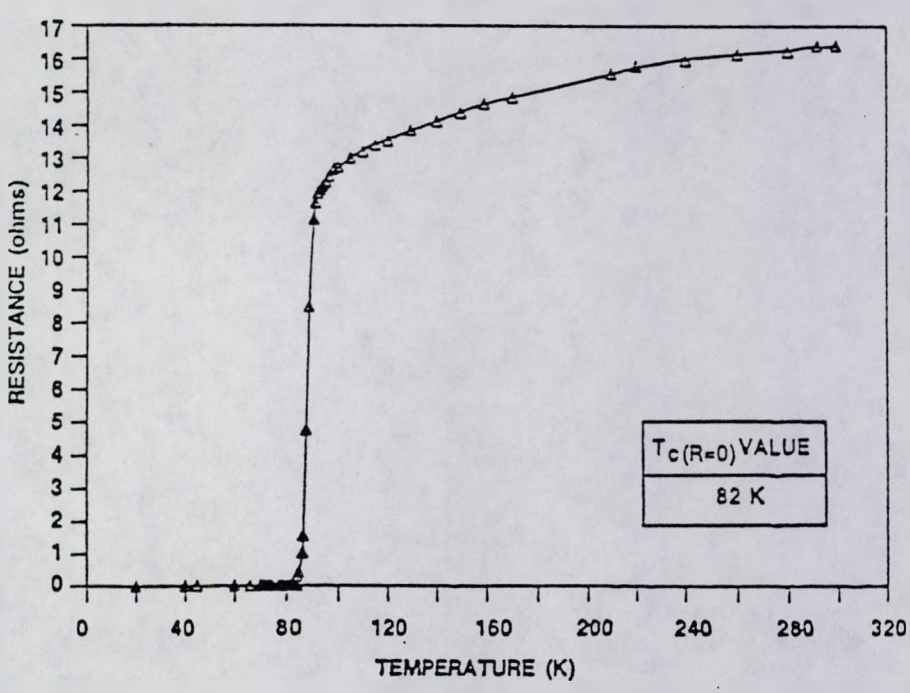

Figure 11. Resistance versus temperature curve for a $YBa_2Cu_3O_x$ coated filament of Saphikon (single crystal Al_2O_3). This sample was coated with a flat MgO substrate, which was also superconducting at 82 K.

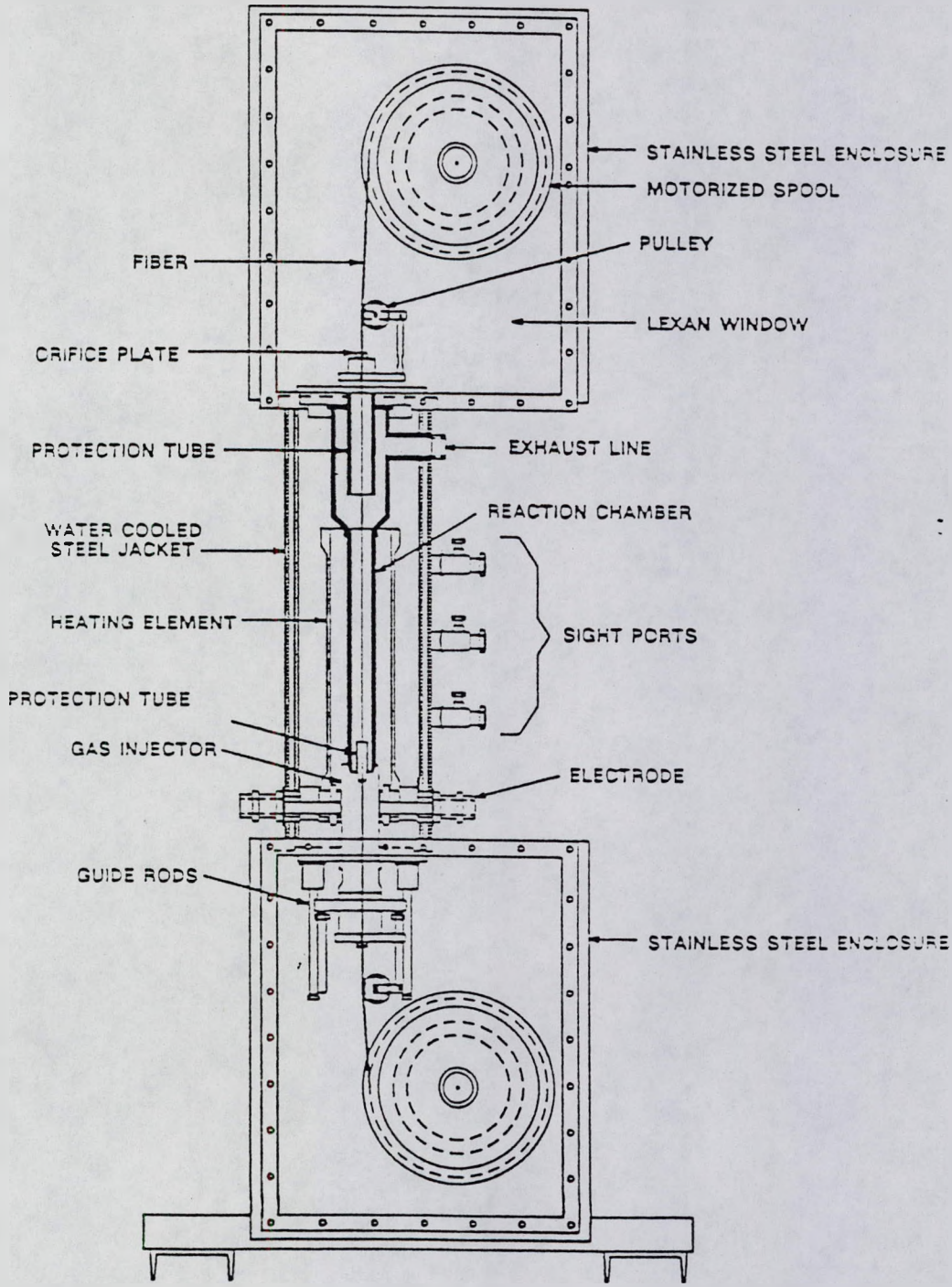

Figure 12. Schematic of the continuous fiber coating furnace.

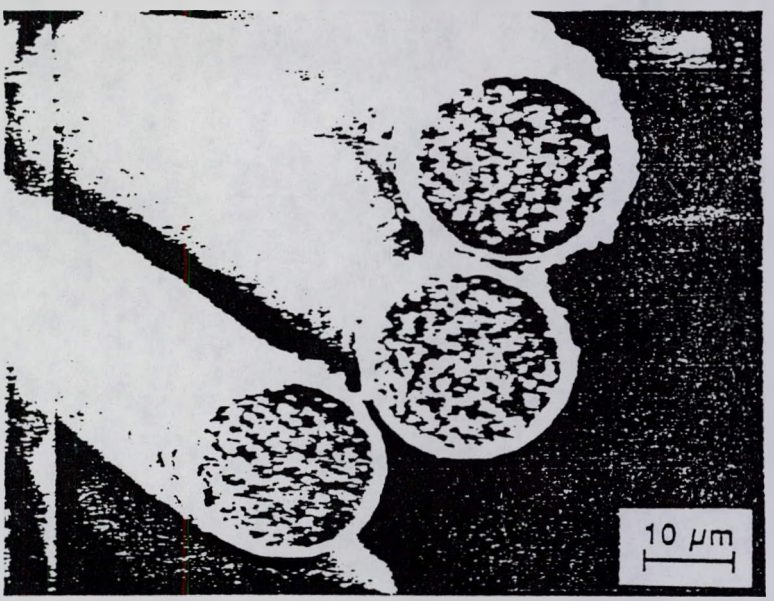

Figure 13. Micrograph of 3 individual filaments from a 200 filament fibrous tow of FP Alumina (Du Pont). EDS confirmed the presence of Y, Ba, and Cu in the coating.